

Formation of a planar coarse wavelength-division multiplexer and demultiplexer with reflection volume phase gratings

Weihong H. Huang, Yaakov Amitai, and Asher A. Friesem

A compact configuration for a coarse wavelength-division multiplexer (CWDM) and a coarse wavelength-division demultiplexer (CWDDM) that are based on reflection volume phase gratings is formed. The design and calculated results for four-channel CWDM and CWDDM configurations in the region near 800 nm are presented. Theoretical predictions are experimentally verified with a four-channel CWDDM whose channels are centered at 775, 800, 825, and 850 nm. © 2002 Optical Society of America

OCIS codes: 050.7330, 060.4230.

1. Introduction

The rapid growth in demand for high-capacity and high-transfer-rate telecommunication links has led to the use of wavelength-division multiplexers (WDMs) and wavelength-division demultiplexers (WDDMs).^{1,2} Such WDMs and WDDMs are devices that either combine a number of optical channels, each of which has a different wavelength, into one composite channel or divide a composite (multiwavelength) channel into different channels according to their wavelengths. In general, the emphasis has been on developing dense WDM (DWDM) and dense WDDM (DWDDM) devices with large numbers of wavelength channels and separation as small as 0.8 nm that are suitable for use in long-haul communication networks. More recently, coarse WDMs (CWDMs) and coarse WDDMs (CWDDMs), with relatively small numbers of wavelength channels and wider separation, typically 10–20 nm, for short-haul and access communication networks are becoming important.³

The current technologies for CWDMs and CWDDMs can be broadly divided into two types: thin-film filter technology and grating-based technology. In the more widespread thin-film filter technology, several discrete thin-film filters are exploited for selecting and separating specific wavelengths.⁴ Typically it is difficult to fabricate such filters because they require a

large number of layers with accurate thickness if they are to yield the desired cutoff spectral profile of the passband, and it is also difficult to align them because of their sensitivity to the input angles. In the grating-based technology, volume phase gratings are exploited to separate specific wavelengths. They are potentially easier to fabricate than the thin-film filters, and, when they are incorporated into planar configurations, alignment problems are greatly alleviated.^{5–9} Most of these configurations involve two gratings, one grating for dispersing and separating wavelength channels and an output grating for coupling the light outward. In general, such grating-based configurations have either nonuniform throughput light efficiency among different wavelength channels or gradual roll-off rather than a cutoff spectral profile. Some are also polarization dependent.

In this paper we develop a different compact planar configuration of grating-based CWDMs and CWDDMs that is formed with several reflection volume phase gratings, each operating independently with a specific wavelength channel. Such CWDMs and CWDDMs could have the desired performance, such as high and uniform throughput light efficiency among different wavelength channels, cutoff spectral profile, arbitrarily selected channel spacing with a specific passband, polarization independence, and low cross talk. Moreover, they are relatively easy to fabricate and replicate.

2. Basic Planar Configuration for the CWDM and the CWDDM

A basic planar configuration for a four-channel CWDM and CWDDM is shown schematically in Fig. 1, where four linear diffraction gratings, parallel to

The authors are with the Department of Physics of Complex Systems, Weizmann Institute of Science, Rehovot 76100, Israel.

Received 5 February 2002; revised manuscript received 10 June 2002.

0003-6935/02/285851-06\$15.00/0

© 2002 Optical Society of America

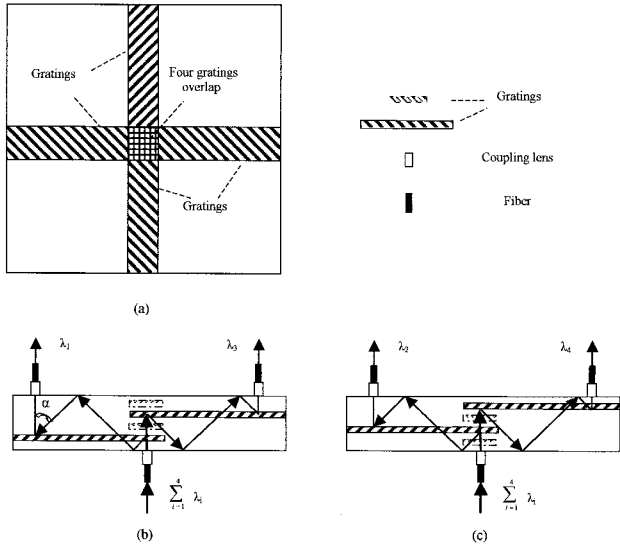


Fig. 1. Planar configuration for a four-channel CWDM and a CWDDM with a single grating for each channel: (a) top view, (b) side view for two channels, (c) side view for the other two orthogonal channels.

one another with an angular orientation of 90° between adjacent gratings, are cascaded inside one substrate. All the gratings are volume phase reflection gratings, each of which was designed to satisfy the Bragg condition for a normally incident input wave of a specific wavelength. We chose reflection, rather than transmission, volume phase gratings because they can provide not only high diffraction efficiency and negligible polarization dependence but also the desired cutoff spectral profile.

In such a CWDDM configuration, light from an input fiber containing channels C_1 , C_2 , C_3 , and C_4 with corresponding wavelengths of λ_1 , λ_2 , λ_3 , and λ_4 is collimated through a coupling lens to form plane waves that are normally incident upon all the gratings. Each grating has a high diffraction efficiency for an incident wave of a specific wavelength and transmits the waves of the other three wavelengths. In particular, only the light from C_1 with wavelength λ_1 is diffracted by the first grating, and, after its propagation inside the substrate, this light will be diffracted out of the substrate by the same grating and coupled into the receiving fiber by a coupling lens. The waves from the other channels, C_2 , C_3 , and C_4 , with wavelengths λ_2 , λ_3 , and λ_4 , will pass the first grating and propagate through the substrate until they are diffracted by their respective gratings afterward and then coupled into their respective fibers in the same way as the light from C_1 . Whether light is diffracted from a specific grating depends on whether the wavelength satisfies the Bragg condition for the volume grating. The waves diffracted from the corresponding gratings will propagate inside a substrate by total internal reflection when angle α is larger than the critical angle, i.e., $\arcsin(1/n_s)$, where n_s is the refractive index of the substrate.

When angle α is chosen to be smaller than the critical angle, the two substrate surfaces must be coated with reflective coatings such that the diffracted light can still propagate inside the substrate by total reflection. Because each wavelength channel is operated by a separate grating, the channel spacing can be chosen as needed, and the efficiency of the throughput light can be independently controlled for each wavelength channel.

Reversing the direction of light causes the output to become the input and the input to become the output such as to form a planar CWDM rather than a CWDDM configuration, in which light waves from separate fibers, each of which has a different wavelength, are coupled into one central composite fiber.

3. Calculated Results and Design Parameters

We start with basic relations of diffraction efficiencies for volume phase reflection gratings to find the needed geometrical and optical parameters to be incorporated into the CWDM and CWDDM devices. According to Kogelnik's theory,¹⁰ diffraction efficiencies η_{\perp} and η_{\parallel} for the TE and the TM polarizations, respectively, for a reflection volume phase grating with normal incident illumination are

$$\begin{aligned}\eta_{\perp} &= \left[1 + \frac{1 - \xi^2/\nu_{\perp}^2}{\sinh^2 \sqrt{\nu_{\perp}^2 - \xi^2}} \right]^{-1}, \\ \eta_{\parallel} &= \left[1 + \frac{1 - \xi^2/\nu_{\parallel}^2}{\sinh^2 \sqrt{\nu_{\parallel}^2 - \xi^2}} \right]^{-1},\end{aligned}\quad (1)$$

where

$$\begin{aligned}\xi &= \frac{\vartheta d}{2Cs}, \quad \nu_{\perp} = \frac{\pi \Delta n d}{\lambda \sqrt{Cs}}, \\ \nu_{\parallel} &= -\frac{\pi \Delta n d}{\lambda \sqrt{Cs}} \cos \alpha, \\ \vartheta &= (1 + \cos \alpha_0) \frac{\beta_0(\beta - \beta_0)}{\beta}, \\ Cs &= \frac{\beta_0}{\beta} (1 + \cos \alpha_0) - 1, \\ \beta &= \frac{2\pi n}{\lambda}, \quad \beta_0 = \frac{2\pi n}{\lambda_0},\end{aligned}\quad (2)$$

where n is the refractive index of the emulsion, Δn is the refractive-index modulation of the grating, d is the grating thickness, $180^\circ - \alpha_0$ is the diffraction angle for Bragg wavelength λ_0 , and $180^\circ - \alpha$ is the diffraction angle for wavelength λ . Using Eqs. (1) and (2), we calculated the diffraction efficiency (DE) of gratings and the channel efficiency (CE) of four-channel CWDDMs as a function of wavelength of different grating parameters. Representative results are presented in Figs. 2–4. The CE is defined as

$$CE = P_{out}/P_{in}, \quad (3)$$

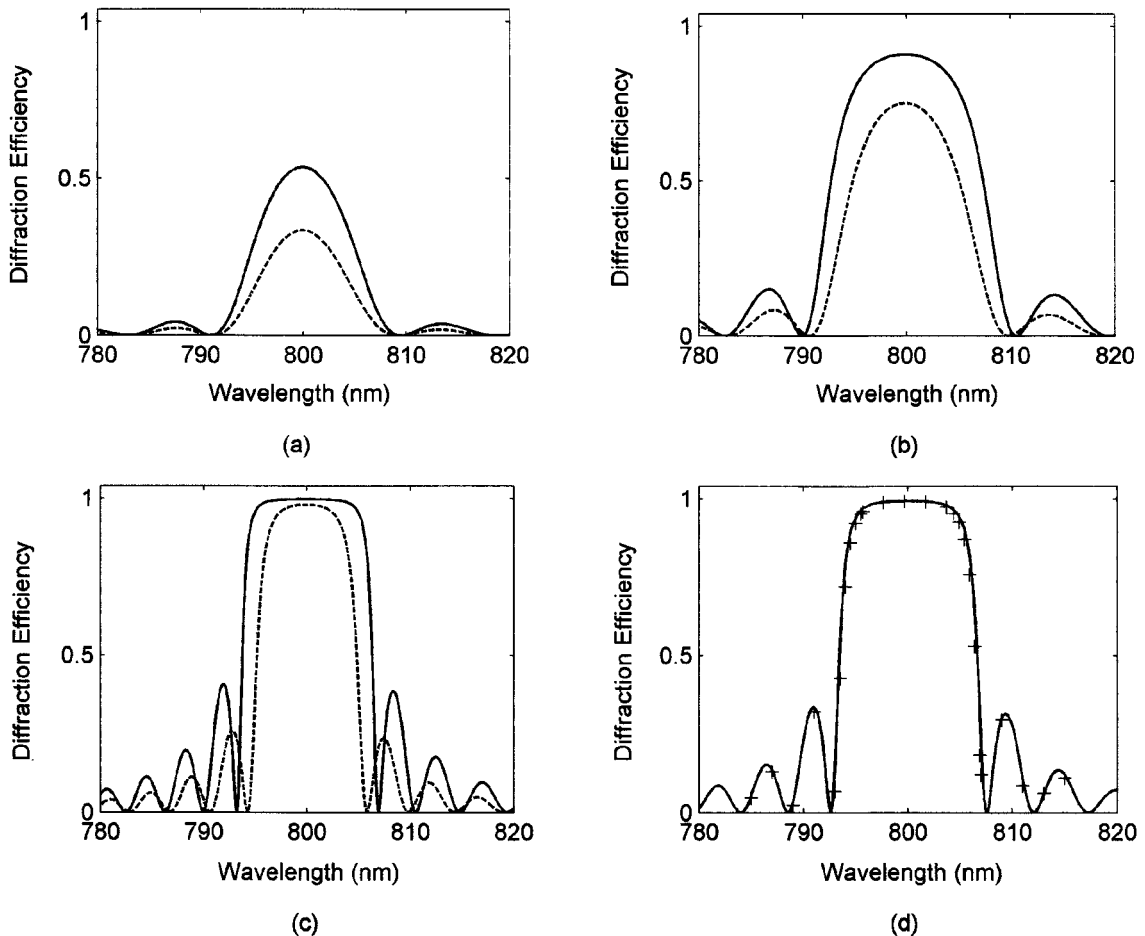


Fig. 2. Calculated diffraction efficiency as a function of wavelength of reflection volume phase gratings: solid curves, for both TE polarizations; dashed curves, for TM polarizations. Grating parameters: (a) $\Delta n = 0.01$, $d = 20 \mu\text{m}$, $\alpha = 45^\circ$; (b) $\Delta n = 0.02$, $d = 20 \mu\text{m}$, $\alpha = 45^\circ$; (c) $\Delta n = 0.02$, $d = 40 \mu\text{m}$, $\alpha = 45^\circ$; (d) $\Delta n = 0.02$, $d = 40 \mu\text{m}$, $\alpha = 15^\circ$.

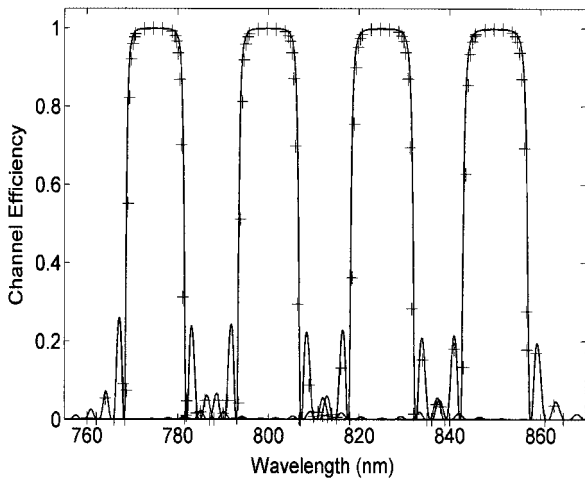


Fig. 3. Calculated channel efficiency as a function of wavelength of a high-performance four-channel CWDDM. Center wavelengths at 775, 800, 825, and 850 nm. Solid curves, TE waves; +, for TM waves. Grating parameters: $d = 50 \mu\text{m}$, $\alpha = 15^\circ$, and $\Delta n = 0.022$.

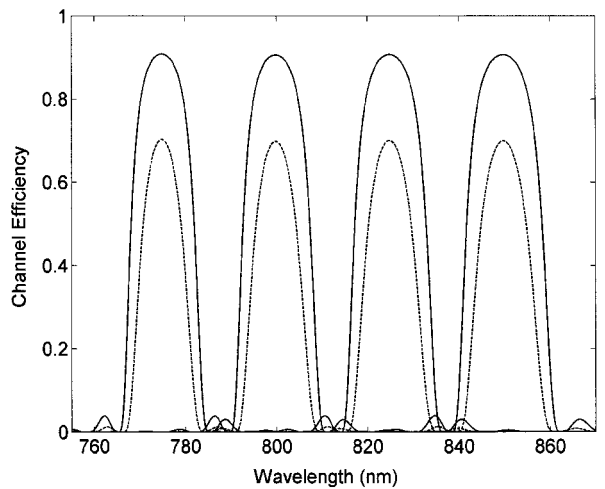


Fig. 4. Calculated channel efficiency as a function of wavelength of a four-channel CWDDM in which the grating parameters are based on available photopolymer recording material. Center wavelengths at 775, 800, 825, and 850 nm. Solid curves, TE waves; dashed curves, for TM waves. Grating parameters: $d = 20 \mu\text{m}$, $\alpha = 45^\circ$, $\Delta n_1 = 0.0229$, $\Delta n_2 = 0.0235$, $\Delta n_3 = 0.0243$, and $\Delta n_4 = 0.0250$ for each channel.

where P_{in} and P_{out} are the input power and the output power, respectively, for the channel. Assuming that all the gratings have uniform DE, the CE is equal to η_{\perp}^2 for TE polarization or to η_{\parallel}^2 for TM polarization, because the input wave of each wavelength channel has to be diffracted by the same grating twice before it is coupled into its corresponding output fiber.

Figure 2 shows the calculated results of DE as a function of wavelength. Figures 2(a)–2(c) show the results for gratings with the same angle $\alpha = 45^\circ$ but different Δn and d : Fig. 2(a) $\Delta n = 0.01$, $d = 20 \mu\text{m}$; Fig. 2(b) $\Delta n = 0.02$, $d = 20 \mu\text{m}$; Fig. 2(c) $\Delta n = 0.02$, $d = 40 \mu\text{m}$. As is evident, the DE is increased significantly when Δn is increased from 0.01 to 0.02 and d from 20 to 40 μm , reaching close to 100% with the desired cutoff spectral profile, as shown in Fig. 2(c). So, for each angle α , we can increase either refractive-index modulation Δn or grating thickness d to achieve high DE with the desired cutoff spectral profile. It should be noted that the DE decreases as the illumination wavelength increases, as indicated in Eqs. (1) and (2). When gratings with a specific d are designed for different wavelength channels, Δn must be varied for uniform CE to be obtained among the various wavelength channels.

The parameters of Δn and d affect not only the DE and the spectral profile but also the spectral passband. Specifically, an increase in refractive-index modulation Δn increases the spectral passband, as one can see by comparing Figs. 2(a) and 2(b), whereas an increase of grating thickness d reduces the spectral passband, as one can see by comparing Figs. 2(b) and 2(c). Thus, for both high DE and the needed passband, grating thickness d and refractive-index modulation Δn must be appropriately selected.

In accordance with Eqs. (1) and (2), angle α influences the dependence of DE on the polarization of the incident light. In particular, diffraction efficiencies η_{\perp} and η_{\parallel} for TE and TM polarization, respectively, are merely functions of ξ^2 and ν^2 . Whereas ξ^2 have the same value for TE and TM polarizations, the values for ν^2 are different, but one can reduce the difference by decreasing angle α . Thus, as angle α is reduced, the dependence of DE and of the spectral passband on the polarization of the incident wave will be decreased. This is evident from a comparison of Figs. 2(c) and 2(d), where angle α was decreased from 45° to 15° .

In general, by properly choosing the three parameters of refractive-index modulation Δn , grating thickness d and angle α , one can obtain reflection volume phase gratings with high diffraction efficiency, desired cutoff spectral profile, needed passband, and polarization independence, such as the one shown in Fig. 2(d). When such gratings are incorporated into our compact four-channel CWDDM configuration, very good results can be obtained. For example, we considered four gratings with the same parameters, $\Delta n = 0.022$, $d = 50 \mu\text{m}$, and $\alpha = 15^\circ$, but different Bragg wavelengths of 775, 800, 825, and 850 nm at normal incidence. With these chosen param-

eters, all four gratings have calculated peak diffraction efficiencies that are close to 100% and have negligible polarization dependence. The CE was calculated as a function of the wavelengths of a four-channel CWDDM formed with these four gratings, and the results are presented in Fig. 3. The calculated maximum cross talk of this CWDDM is -23.0 dB , where the cross talk of the CWDDM is defined as the ratio of the light arriving from all unwanted wavelength channels to that of the wanted wavelength channel.

In practice, however, there are some limitations that must be imposed on refractive-index modulation Δn , grating thickness d , and angle α . For example, the refractive-index modulation for a typical volume phase recording medium, such as a commercial photopolymer, can be only as high as 0.025. The available thickness of such photopolymers is only 20 μm , although experimental photopolymer recording media with thicknesses of several centimeters have been reported.¹¹ Finally, angle α must be larger than the critical angle, i.e., $\arcsin(1/n_s) = 41.8^\circ$, with $n_s = 1.5$, if the surfaces of the substrate have not been coated with reflective coating.

We considered a four-channel CWDDM in which the parameters of the four gratings are available with commercial photopolymer recording material and no reflective coating is needed. Specifically, the four gratings have the same parameters, $d = 20 \mu\text{m}$ and $\alpha = 45^\circ$, but different values of Δn , i.e., $\Delta n_1 = 0.0229$, $\Delta n_2 = 0.0235$, $\Delta n_3 = 0.0243$, and $\Delta n_4 = 0.0250$, and different Bragg wavelengths 775, 800, 825, and 850 nm at normal incidence. The calculated results of the CE as a function of wavelength for this CWDDM are presented in Fig. 4. The maximum cross talk of this CWDDM was calculated as -21.1 dB .

We also calculated the performance of a single channel centered at a wavelength of 800 nm that was incorporated into a CWDDM with selected grating parameters $d = 50 \mu\text{m}$ and $\alpha = 15^\circ$ or into a CWDDM with grating parameters $d = 20 \mu\text{m}$ and $\alpha = 45^\circ$. Specifically, we determined the minimum insertion loss, passband, and figure of merit (FOM). The insertion loss is defined as $-10 \log \text{CE}$, and the passband is determined as the spectral bandwidth of the DE response at the insertion loss of 25 dB. Finally, the FOM, which characteristically is the sharpness of the cutoff in the spectral profile, is defined as

$$\text{FOM} = \frac{(\lambda_2 - \lambda_1)_{\text{at } 0.5 \text{ dB}}}{(\lambda_2 - \lambda_1)_{\text{at } 20 \text{ dB}}}, \quad (4)$$

where the insertion loss at $(\lambda_2)_{\text{at } 0.5 \text{ dB}}$ or at $(\lambda_1)_{\text{at } 0.5 \text{ dB}}$ equals the minimum insertion loss plus 0.5 dB, whereas the insertion loss at $(\lambda_2)_{\text{at } 20 \text{ dB}}$ or at $(\lambda_1)_{\text{at } 20 \text{ dB}}$ equals the minimum insertion loss plus 20 dB. The calculated results are presented in Table 1. As is evident from Table 1 as well as from Figs. 3 and 4, one can significantly improve the performance of the CWDDM with grating parameters based on available photopolymer recording material by resorting to

Table 1. Calculated Performance of a Single Channel Centered at 800 nm for Four-Channel CWDDMs with Different Grating Parameters

| Performance Parameter ^a | Grating Parameters | |
|------------------------------------|---|---|
| | $d = 50 \mu\text{m}$, $\alpha = 15^\circ$ | $d = 20 \mu\text{m}$, $\alpha = 45^\circ$ |
| Minimum insertion loss for TE | 0.005 dB | 0.431 dB |
| Minimum insertion loss for TM | 0.007 dB | 1.560 dB |
| Passband for TE | 14.41 nm | 21.57 nm |
| Passband for TM | 14.10 nm | 19.72 nm |
| FOM for TE | 0.933 | 0.750 |
| FOM for TM | 0.926 | 0.582 |

^aTE, the input light was TE polarized; TM, the input light was TM polarized.

grating parameters that are specially chosen based on our theoretical analysis.

4. Experimental Procedure and Results

To verify our predictions we designed and recorded four gratings with parameters of $d = 20 \mu\text{m}$ and $\alpha = 45^\circ$ for a four-channel CWDDM with central wavelengths at 775, 800, 825, and 850 nm. The recording material was DuPont HRF-700X314 photopolymer, which is a blue/green-light sensitive, reflection-type film with a thickness of $20 \mu\text{m}$.^{12,13} The gratings were holographically recorded with the 488-nm wavelength derived from an argon laser. The recording angles were calculated to satisfy the Bragg condition for the readout angles and wavelengths. To form a CWDDM of the configuration shown in Fig. 1 we first recorded four independent gratings, each for a different wavelength channel, upon separate substrates.

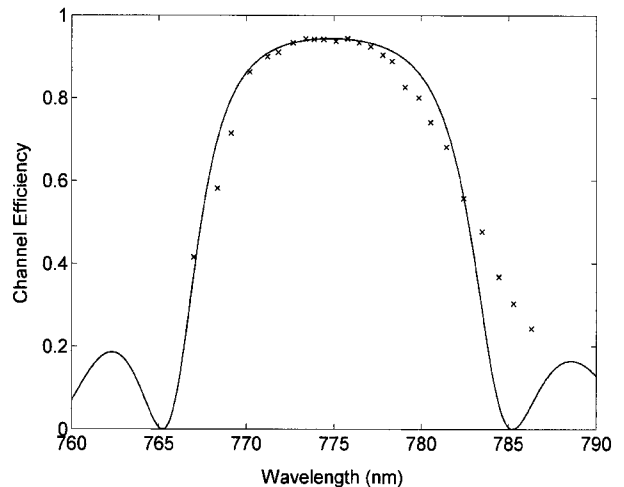


Fig. 6. Experimental and calculated channel efficiency as a function of wavelength of a single wavelength channel centered at 775 nm when the input light was TE polarized. Solid curve, results calculated with $d = 20 \mu\text{m}$, $\Delta n = 0.022$, and $\alpha = 45^\circ$; \times , experimental measurements.

The four substrates with recorded gratings were then attached in a series with optical glue; we ensured that adjacent gratings were rotated 90° with respect to each other. The overall size of the experimental CWDDM device was approximately $0.4 \text{ cm} \times 2 \text{ cm} \times 2 \text{ cm}$, and the distance from each output to the input was 1.6 cm.

Representative results for the four-channel CWDDM are presented in Figs. 5 and 6 and Table 2. Figure 5 shows the output intensities of the four-

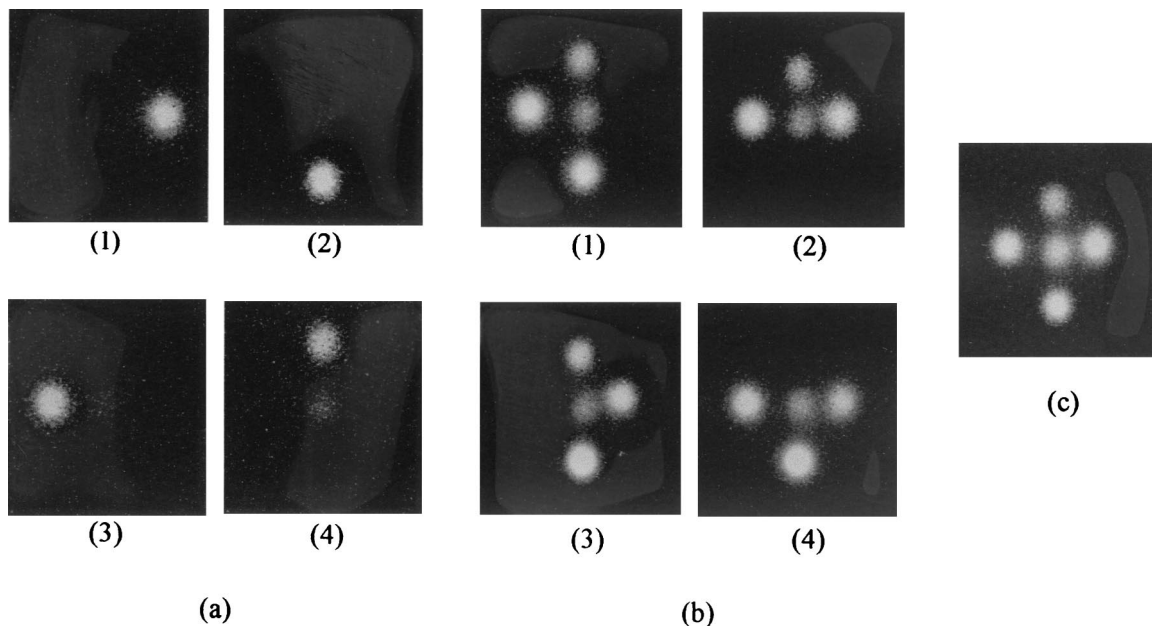


Fig. 5. Detected output intensities of the four-channel CWDDM. (a) Input light of a single wavelength: (1) 775 nm, (2) 802 nm, (3) 824 nm, (4) 849 nm. (b) Input light of three wavelengths: (1) 802, 824, and 849 nm; (2) 775, 824, and 849 nm; (3) 775, 802, and 849 nm; (4) 775, 802, and 824 nm. (c) Input light of four wavelengths: 775, 802, 824, and 849 nm. The middle spots depict directly transmitted nondiffracted light.

Table 2. Experimental Performance of a Four-Channel CWDDM Recorded with DuPont HRF-700X314 Photopolymer with $d = 20 \mu\text{m}$ and $\alpha = 45^\circ$

| Performance Parameter ^a | Nominal Central Wavelength | | | |
|------------------------------------|----------------------------|--------------------|--------------------|--------------------|
| | Channel 1 (775 nm) | Channel 2 (800 nm) | Channel 3 (825 nm) | Channel 4 (850 nm) |
| Measured central wavelengths | 775 nm | 802 nm | 824 nm | 849 nm |
| Peak CE for TE | 0.900 | 0.846 | 0.839 | 0.787 |
| Peak CE for TM | 0.692 | 0.648 | 0.642 | 0.543 |
| Minimum insertion loss for TE | 0.47 dB | 0.72 dB | 0.76 dB | 1.04 dB |
| Minimum insertion loss for TM | 1.60 dB | 1.88 dB | 1.93 dB | 2.65 dB |
| Maximum cross talk | -20.7 dB | | | |

^aTE, the input light was TE polarized; TM, the input light was TM polarized.

channel CWDDM as detected by a digital camera. Figure 5(a) shows the detected output intensity as the wavelength of input light was varied from 775 nm to 802, 824, and 849 nm. As expected, the output light's position changed in accordance with the input wavelength. Figure 5(b) shows the detected output intensity when the input light comprises three wavelengths simultaneously. As expected, three dominant spots were detected, each depicting light from a different wavelength channel. The fourth, weaker, spot at the center depicts nondiffracted light that passed directly through the CWDDM. We found that the cross talk is too small to be detected by the camera. Finally, Fig. 5(c) shows the detected output intensity when the input light comprises all four wavelengths simultaneously. Now, as expected, there are four dominant spots, each depicting light from a different wavelength channel. The middle (fifth) spot again depicts the nondiffracted light.

Table 2 presents the experimental central wavelength, peak CE, and corresponding minimum insertion loss at each wavelength channel as well as the maximum cross talk of the CWDDM. The channel efficiency was measured as the intensity of the output light from a channel divided by the intensity of the light directly transmitted through a clear part of the substrate on which no grating is present. We determined the maximum cross talk of the CWDDM by measuring the output intensity at the location of a certain wavelength channel, first when the input light was of a corresponding wavelength and then when it simultaneously comprised the three other wavelengths. Finally, Fig. 6 shows the experimental and calculated channel efficiency as functions of wavelength for a single wavelength channel centered at 775 nm that uses a tunable semiconductor laser. The input light was TE polarized. As is evident, the experimental results are in reasonable agreement with the theoretical predictions, for which the parameters $d = 20 \mu\text{m}$, $\alpha = 45^\circ$, and $\Delta n = 0.022$ were assumed.

5. Concluding Remarks

A compact configuration for coarse wavelength-division multiplexers and coarse dense wavelength-division multiplexers based on reflection volume phase gratings that operate independently on specific

wavelength channels was developed. Calculated results indicate that high and uniform channel efficiencies, desired cutoff spectral profiles, low cross talk, and polarization independence can be achieved. Some of the calculated results were successfully verified with an experimental four-channel CWDDM operating near 800 nm. By using a thicker phase recording material and a different grating recording geometry or wavelength it should be possible to use the same CWDM and CWDDM configuration in the wavelength region near 1550 nm.

References

1. L. Kazovsky, "Multichannel systems," in *Optical Fiber Communication Systems*, S. Benedetto and A. Willner, eds. (Artech House, Norwood, Mass., 1996), pp. 513–616.
2. H. Taga, "Long distance transmission experiments using the WDM technology," *J. Lightwave Technol.* **14**, 1287–1298 (1996).
3. J. J. Petiote, "Low-cost components give coarse WDM an edge," in *WDM Solutions* (January 2001), pp. 47–51.
4. J. Minowa and Y. Fuji, "Dielectric multilayer thin-film filters for WDM transmission systems," *J. Lightwave Technol. LT-1*, 116–121 (1983).
5. Y. T. Huang, D. C. Su, and Y. K. Tsai, "Wavelength-division-multiplexing and -demultiplexing by using a substrate-mode grating pair," *Opt. Lett.* **17**, 629–1631 (1992).
6. M. M. Li and R. T. Chen, "Five-channel surface-normal wavelength-division demultiplexer using substrate-guided waves in conjunction with a polymer-based Littrow hologram," *Opt. Lett.* **20**, 797–799 (1995).
7. Y. K. Tsai, Y. T. Huang, and D. C. Su, "Multiband wavelength-division demultiplexing with a cascaded substrate-mode grating structure," *Appl. Opt.* **34**, 5582–5588 (1995).
8. Y. Amitai, "Design of wavelength-division multiplexing/demultiplexing using substrate-mode holographic elements," *Opt. Commun.* **98**, 24–28 (1993).
9. Y.-K. Tsai, Y.-T. Huang, and D. C. Su, "A reflection-type substrate-mode grating structure for wavelength-division multi/demultiplexing," *Optik (Stuttgart)* **97**, 62–69 (1994).
10. H. Kogelnik, "Coupled wave theory for thick hologram gratings," *Bell Syst. Tech. J.* **48**, 2909–2947 (1969).
11. L. Dhar and A. Hale, "Recording media that exhibit high dynamic range for digital holographic data storage," *Opt. Lett.* **24**, 487–489 (1999).
12. B. L. Booth, "Photopolymer material for holography," *Appl. Opt.* **14**, 593–601 (1975).
13. W. K. Smothers, B. M. Monroe, A. M. Weber, and D. E. Keys, "Photopolymers for holography," in *Practical Holography IV*, S. A. Benton, ed., *Proc. SPIE* **1212**, 20–29 (1990).